



International Journal of Proteomics & Bioinformatics

Research Article

The classification of HIV and non-HIV related DLBCL subtypes using MALDI Imaging Mass Spectrometry -

Pumza Magangane[#], Raveendra Sookhayi[#] and Richard Naidoo^{*}

Division of Anatomical Pathology, Department of Pathology, University of Cape Town/ National Health Laboratory Services, Cape Town 7925, South Africa

#Equal contribution

***Address for Correspondence:** Division of Anatomical Pathology, Department of Pathology, University of Cape Town/ National Health Laboratory Services, Cape Town 7925, South Africa, Tel: +271-148-988-82; E-mail: Richard.Naidoo@uct.ac.za

Submitted: 28 November 2018; Approved: 15 December 2018; Published: 19 December 2018

Cite this article: Magangane P, Sookhayi R, Naidoo R. The classification of HIV and non-HIV related DLBCL subtypes using MALDI Imaging Mass Spectrometry. *Int J Proteom Bioinform.* 2018;3(1): 010-015.

Copyright: © 2018 Naidoo R, et al. This is an open access article distributed under the Creative Commons Attribution License, which permits unrestricted use, distribution, and reproduction in any medium, provided the original work is properly cited.

ABSTRACT

Background: Matrix-Assisted Laser Desorption/Ionization Imaging Mass Spectrometry (MALDI IMS) is a powerful technology which determines the localization of proteins directly on tissue sections. This technology can also be used to classify distinct disease entities. Diffuse Large B Cell Lymphoma (DLBCL) is a heterogeneous disease that is subdivided into Germinal Centre (GC) and non-GC subtypes using immunohistochemical staining. The diagnosis, management and treatment of the disease may benefit from molecular classification of the tissue as new target proteins can be identified.

Methods: The tissue samples included Germinal Centre (GC) subtypes (n = 3), (n = 4) and non-GC subtypes (n = 4), (n = 4) from HIV negative and positive cases, respectively. Classification models were created and validated with an independent set of tissue from GC (n = 2) and non-GC (n = 2) subtypes for both HIV negative and HIV positive cohorts, respectively.

Results: In the HIV negative cohort, we found that 27 proteins were differentially expressed in GC compared to non-GC. The generated classification model based on the most significant 8 differentially expressed proteins allowed for reliable prediction of subtype in the validation set with a prediction score of 100%. The HIV positive cohort had a lower number of differentially expressed peptide ions which were all included in the classification model. This model was not as reliable as the HIV negative model which had a prediction score of 79%.

Conclusions: The classification models identified herein may be used in routine diagnostics so to confirm the subtype status of DLBCL patients.

Keywords: MALDI IMS; DLBCL; Classification; proteomics; Subtypes

ABBREVIATIONS

MALDI IMS: Matrix Assisted Laser Desorption/Ionization Imaging Mass Spectrometry; DLBCL: Diffuse Large B Cell Lymphoma; HIV: Human Immunodeficiency Virus; GC: Germinal Centre; HSP: Heat Shock Protein; TIC: Total Ion Current; GA: Genetic Algorithm; NHL: Non-Hodgkin Lymphoma; GEP: Genetic Expression Profiling; FFPE: Formalin Fixed Paraffin Embedded

BACKGROUND

Personalized cancer therapy and disease prognosis relies on accurate classification of the tumor. At present, histopathological diagnosis is based on information from the clinic, morphological and immunophenotypic assessments, and occasionally, molecular tests. This process is time consuming and offers limited biological or molecular understanding of the disease. Molecular classification aims to emphasize the molecular heterogeneity of tumors so as to determine markers to improve diagnosis, prognosis, and treatment efficacy. Matrix Assisted Laser Desorption/Ionization (MALDI) Imaging Mass Spectrometry (IMS) is a powerful technology which investigates the molecular content of tissues while preserving their morphological structure [1]. The MALDI IMS technology has various applications including; molecular classification of tissue, analysis of intra-tumour diversity and determining drug metabolism kinetics [2-4]. This technology has been applied for molecular classification purposes in several cancers including melanoma [5], breast cancer [6,7] and pancreatic cancer [8]. Casadonte et al. successfully used MALDI IMS to discriminate breast cancer from pancreatic cancer metastasis. Djidja and his group created a model that may be used to classify pancreatic tumour from normal tissue and adenocarcinomas.

Diffuse Large B Cell Lymphoma (DLBCL) is the most commonly diagnosed Non-Hodgkin Lymphoma (NHL) subtype, comprising of more than a third of NHL cases [9,10]. It is heterogeneous in nature, with morphological, molecular and genetic subtypes [11]. Genetic Expression Profiling (GEP) classifies DLBCL into subtypes based on their 'cell of origin' phenotype. [12] Classified DLBCL into Germinal Centre (GC) and Activated B Cell (ABC) subtypes. The GEP technology is not readily accessible to most hospitals due to specialised training and high costs involved. As a result, various

immunohistochemistry based classification methods have been developed to model the GEP classification scheme [13-15]. Some of these have high concordance with GEP and are currently used at clinical settings [13,15]. Given the heterogeneity of DLBCL, we thought it would benefit from the technology of MALDI IMS as it may be used in disease subtyping and possibly even discrimination from other types of high grade B cell lymphomas.

In this study, we propose a classification model that may be used either in conjunction with the immunohistochemistry-based algorithms or as a standalone for subtyping of DLBCL cases.

MATERIALS AND METHODS

Materials used

All reagents were bought from Sigma-Aldrich (Merck KGaA, Darmstadt, Germany) unless otherwise stated.

Sample details

The study was only limited to twenty three DLBCL Formalin Fixed Paraffin Embedded (FFPE) tissue samples, due to financial constraints. All the samples were collected at the Groote Schuur Hospital in Cape Town, South Africa. The diagnosis of DLBCL was based on the WHO criteria for morphology and immunostaining. Burkitt's lymphoma and plasmablastic lymphomas were excluded based on morphology and immunolabeling. The grey zone lymphomas, bordering between a Burkitt's lymphoma and DLBCL, and Hodgkin's lymphoma and DLBCL were also excluded. DLBCL samples obtained from HIV infected (n = 8) and HIV uninfected patients (n = 7) were used as a test set.

The validation cohort consisted of cases from HIV infected (n = 4) and HIV uninfected (n = 4) DLBCL patients (Table S1). The tissue from the validation cohort was handled and processed in the exact manner as the main cohort.

Tissue preparation for MALDI IMS

The FFPE tissues were prepared for MALDI IMS analysis using a workflow our laboratory developed. Briefly, tissue blocks were sectioned at 10 µm and placed onto poly-L- coated ITO slides. Tissue sections were then dewaxed with xylene and cleared with graded



ethanol washes. Trypsin (Promega, Madison USA) solution (5 ng/μl in 50% acetonitrile; 50 mM ammonium bicarbonate, pH 8) was deposited onto tissue sections using the ‘Trypsin deposition’ method on the Bruker Imageprep instrument. Digestion occurred for 15 hours at 37°C. The tissue sections were then coated with matrix (7 g/l in 60% acetonitrile, 0.2% trifluoroacetic acid) prior to MALDI IMS analysis UltrafleXtreme MALDI-TOF/TOF mass spectrometer instrument. Mass spectra were acquired at a spatial resolution of 100 μm in reflectron mode. Ions were collected for the mass range of m/z 700- 3500.

MALDI IMS data analysis

MALDI IMS generates a large amount of data per sample. Therefore, only a limited number of mass spectra from tumour regions in the sections were exported for subsequent statistical analysis using ClinProTools software. The data from both the discovery and validation cohort were analyzed using the same settings. A hundred (100) randomly chosen spectra from each sample were compared between the two DLBCL subtypes. Spectral pre-processing included TopHat baseline correction, and TIC normalization. The Genetic Algorithm (GA) model was used for classification. The k-nearest neighbor parameter in the algorithm setting was set to 3.

nLC-MS/MS analysis for protein identification

The tissue sections were washed in 70% ethanol to remove matrix. They were then subjected to *in situ* trypsin digestion. The extraction of the peptides was carried out using 20 μl of 10% Acetonitrile. The acetonitrile was pipette up and down the entire tissue section. The extract was then concentrated to 2 μl and taken through a C18 zip tip. Seven microliters were subjected to separation on an EASY-nLC II connected to a Proteineer fc II protein spotter controlled through HyStar software. Peptide separation was performed on a EASY column (2 cm, 75 μm ID, 5 μm, C18) followed by an analytical column (10 cm, 75 μm ID, 3 μm, C18) with a flow rate of 100 μl/hr using a 48 minute gradient run. Fractions were collected on a Bruker MTP 384 AnchorChip target (Bruker Daltonics, Bremen, Germany). MALDI-TOF MS and LIFT MS/MS were acquired for all fractions on a Bruker UltrafleXtreme MALDI-TOF/TOF mass spectrometer (Bruker Daltonics, Bremen, Germany). Peptides were ionized with a 337 nm laser and spectra acquired in reflector positive mode at 28kV using 100 laser shots per spectrum with a scan range of m/z 700 -4000. Spectra were internally calibrated using peptide calibration standard II (Bruker Daltonics, Bremen, Germany). Peptide spectra of accumulated 4,000 shots were automatically processed using WARP LC 3.2 software (Bruker Daltonics, Bremen, Germany). Database interrogation was performed with the Mascot algorithm using the SwissProt database on a ProteinScape 3.0 workstation. The *Homo sapiens* and Viruses databases were searched using the following parameters: enzyme specificity was set to trypsin allowing for a missed cleavage of 1. Carbamidomethyl was set as a fixed modification and oxidation as a variable modification. The maximum allowed mass deviation was set to 50 ppm for monoisotopic precursor ions and 0.7 Da for fragments.

RESULTS

Spectra randomly chosen from the tumour region of each sample were exported and compared (Figure S1). There were 27 peptide ions which were differentially expressed between the GC and non-GC subtypes in the HIV negative cohort (Table 1). The differentially expressed peptide ions in each cohort were used to

generate a classification model distinguishing between GC and non-GC subtypes for each HIV cohort. The most discriminatory peptide ions were included in the model and were given different weightings. The model distinguishing between the DLBCL subtypes of the HIV negative cohort contained nine peptide ions (Table 2). These had 100% recognition ability within the test set and 100% ability score to

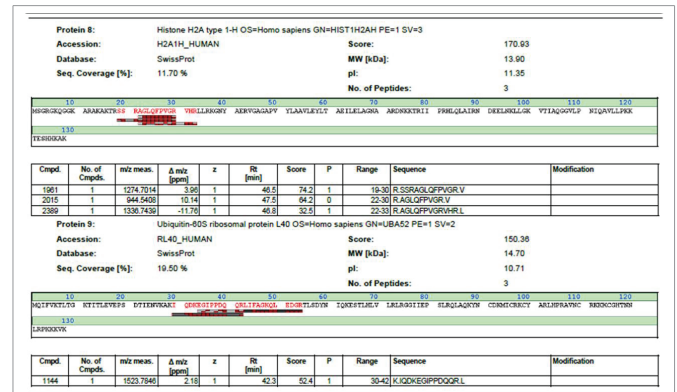


Figure S1: An extract of the swissprot report showing the peptides identified, scores and where they matched to the protein sequence.

Table 1: The differentially expressed peptide ions between germinal centres and non-GC of DLBCL in HIV negative cases and HIV positive cases.

GC/non-GC-	Regulation pattern	GC/non-GC+	Regulation pattern
713.5531	Up	788.71	Up
757.6075	Up	789.71	Up
788.6508	Up	805.72	Up
789.641	Up	928.78	Up
801.6496	Up	944.797	Up
805.6532	Up	945.78	Up
816.6384	Down	1032.93	Up
836.6418	Down	1039.35	Up
845.3651	Up	1105.56	Down
848.605	Down	1199.16	Up
849.6152	Down		
850.6619	Down		
861.2948	Up		
898.6963	Down		
940.7182	Up		
944.7667	Up		
945.7494	Up		
957.7619	Up		
966.7403	Up		
971.7643	Up		
978.8001	Up		
988.7306	Up		
1032.823	Up		
1039.766	Up		
1105.822	Down		
1199.041	Up		
1792.199	Down		



correctly predict the validation set (Table 4). The peptide ions with the highest weighting were m/z 1105.82 (annexin 5), m/z 1199.04 (heat shock protein 70), m/z 1032.82 (histone H3).

The HIV positive cohort only contained ten differentially expressed peptide ions between the same groups (Table 1). The classification model distinguishing between DLBCL subtypes in the HIV positive cohort also contained nine peptide ions (Table 3). The peptide ions with the highest weighting were m/z 928.78, m/z 1032.92 (histone H3), m/z 1039.85 (60S ribosomal protein L40). The model had a high ability to correctly predict subtype when used within the test set, however this was decreased to 79% when using the validation set (Table 4).

DISCUSSION

Our study determined a classification model that enables differentiation between HIV and non-HIV related DLBCL subtypes. Previous studies using MALDI MS for classification purposes did not identify the peptide ions contained in their developed models. Our study utilises MALDI IMS together with peptide identification to classify DLBCL subtypes. The two classification models calculated

Table 2: The model generated from the GC v/s non-GC comparison set of the HIV negative cohort.

Mass	Weight	Identity
1105.82	2.0036	Annexin 5
1199.04	1.2543	Heat shock protein 70
1032.82	1.014	Histone H3
850.66	0.7533	Histone H2A
971.76	0.46277	
988.73	0.6916	
805.65	0.2335	GAPDH
957.76	0.4524	Enolase A
816.64	0.7786	Histone H2B

Table 3: The model generated from the GC and non-GC comparison set of the HIV positive cohort.

Mass (m/z)	Weight	Identity
945.78	1.34801	Histone H2A
1032.92	1.6253	Histone H3
1199.14	1.06205	Heat shock protein 70
1039.85	1.3899	60S ribosomal protein L40
788.71	1.2026	Histone H3
789.7	1.1877	40S ribosomal protein S16
928.78	2.2185	
944.82	1.3055	Histone H2A
1105.84	1.02309	Annexin 5

Table 4: The recognition and validation values of genetic algorithm model generation and validation.

Comparison set	Recognition Ability	Cross Validation	External Validation
GC and non-GC, HIV-	100%	98.5%	100%
GC and non-GC, HIV+	100%	100%	79.4%

Table S1: The baseline characteristics of the cases used for MALDI IMS analysis.

	Test Set		Validation set	
	HIV - DLBCL	HIV + DLBCL	HIV - DLBCL	HIV + DLBCL
Number of cases	7	8	4	4
Age (Yrs)	59.3	39.25	54.75	38.5
Gender (F:M)	5:2	5:3	3:1	3:1
Non-GC Subtypes				
Age	61	34.25	63	34.3
Gender	2:2	3:1	1:1	2:0
GC subtype				
Age	57	44.25	46.5	42.5
Gender	3:0	2:2	2:0	1:1

had similar proteins which points to the similarities of the disease in both HIV contexts. The differences observed between the two DLBCL models may be due to HIV infection or due to differences in the concentrations of peptide ions (Figure 1A & 1B).

The peptides that formed part of the classification models were identified using LC-MS/MS. However, not all peptides could be identified due to differences in the ionisation techniques [16]. The proteins highlighted in this study have previously been implicated in tumourigenesis as well as having a role in prognosis.

GAPDH forms part of the glycolytic pathways but is also involved in several other cellular processes such as, apoptosis and proliferation [17]. A study by Chiche et al. observed that overexpression of GAPDH is associated with aggressiveness (measured as poor prognosis) and vascularisation of non-Hodgkin's lymphoma tumours, via HIF-1 induction by NF- κ B. GAPDH was overexpressed in the more aggressive non-GC subtype (Table 1), which has a constitutively active NF- κ B pathway, thus suggesting a mechanism for the aggressive behaviour of this subtype [18]. The prolonged expression of NF- κ B has been hypothesised to be responsible for the tumour aggressiveness of the non-GC subtype [18,19].

Enolase, a plasminogen receptor, is involved in concentrating proteolytic plasmin activity on the cell surface of haematopoietic and endothelial cells, suggesting a role in regeneration, immune response and metastasis [20-22]. Studies have shown that an upregulation of enolase results in cancer invasion and provides therapy resistance [23-25]. Our study observed an upregulation of enolase in the non-GC subtype of the HIV negative group (Table 1), suggesting that resistance to therapy may possibly be a reason to explain poor prognosis in this subtype.

Heat Shock Proteins (HSP) are a family of proteins produced by cells in response to stress [26]. Levels of the HSP are elevated in many cancers [27,28]. The over-expression of HSP signals a poor prognosis and poor response to therapy [30]. HSP70 (m/z 1199) was elevated in the non-GC group (Table 1), suggesting its involvement in this group showing advanced stage disease.

Ribosomal proteins are commonly upregulated in cancer [30,31]. They are said to participate in tumourigenesis by their extra ribosomal functions [32,33]. Although the ribosomal protein (m/z 789 and m/z 1039) were differentially expressed in both cohorts, they only have a discriminatory role in the HIV positive group. The overexpression of ribosomal protein L40 (m/z 1039) has been shown to play a role

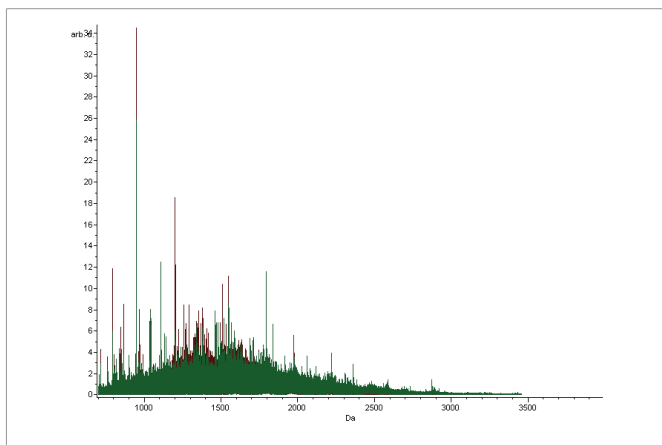


Figure 1A: The average spectrum from the GC (green) and non- GC (red) subtypes of DLBCL in HIV negative patients.

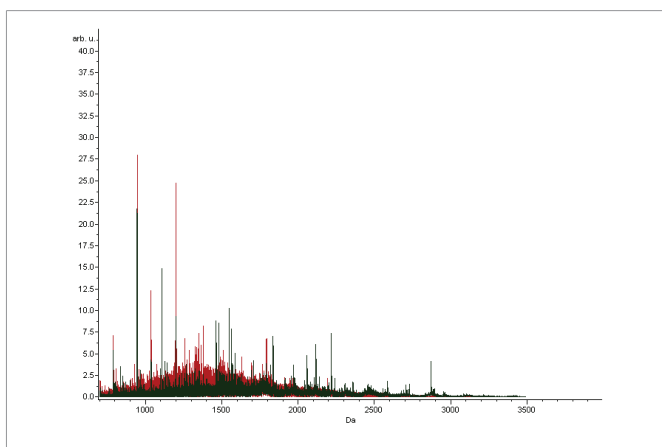


Figure 1B: The average spectrum from the GC (green) and non- GC (red) subtypes of DLBCL in HIV positive patients.

in tumourigenesis and tumour aggressiveness [34,35]. Therefore, the high weighting related to this protein in the model may signify a role in the tumour aggressiveness of the non-GC subgroup.

The proteins mentioned above show an increased expression in the non-GC subtype in both contexts and may be involved in the aggressiveness of this subtype.

The various histone protein families that are commonly isolated in MALDI IMS experiments [5,8,36] may be due to the technical limitations associated with MALDI IMS which favours both high abundant and soluble proteins [37]. The histone proteins were highly weighted in both cohorts, signifying their importance in the classification model. Specifically, histone H3 and H2A had high weightings which allowed discrimination between GC and non-GC subtypes (Table 2 and Table 3). Expression of histone H4, H2B, and H3 were found to positively correlate with patient survival in melanoma lymph node metastases [35]. Increased expression of histone H2A and H3 were observed in the GC subtype in both HIV context, suggesting an involvement in the favourable prognosis experienced by this group.

The proteins identified in this study have previously been implicated in tumourigenesis as well as having a role in prognosis. Therefore, further research is warranted on the potential targeting of these proteins for treatment.

CONCLUSIONS

This study developed protein classification models that discriminates between GC and non-GC subtypes of DLBCL in both HIV and non-HIV contexts. The accuracy of these models was tested on a separate cohort with high predictive power, especially in the HIV negative group. In addition, we have extrapolated the m/z mass ions in the model for protein identification. Finally, we also showed that MALDI IMS can be used to correctly classify DLBCL subtypes. This technology may be used together with routine diagnostics to confirm DLBCL subtypes.

FUNDING

The work was supported by grants from the National Research Foundation (Grant number 91571), National Health Laboratory Service Research Trust (Grant number GRANT004_94441) and the University of Cape Town.

ETHICS APPROVAL

The project was approved by the University of Cape Town, Faculty of Health Sciences Human Research Ethics committee (HREC REF: 261/2010).

AUTHOR'S CONTRIBUTIONS

PM carried out the proteomic studies, performed the statistical analysis and drafted the manuscript. RS reviewed the diagnosis of each case and carried out the selection of cases included in the study. RN conceived of the study, provided the financial support and participated in its design and coordination in addition to drafting the manuscript. All authors read and approved the final manuscript.

ACKNOWLEDGEMENTS

We thank Padmini Govender for the sectioning of FFPE tissue blocks.

REFERENCES

- Balluff B, Rauser S, Meding S, Elsner M, Schone C, Feuchtinger A, et al. MALDI imaging identifies prognostic seven-protein signature of novel tissue markers in intestinal-type gastric cancer. *Am J Pathol.* 2011; 179: 2720-2729. <https://goo.gl/6qFuTm>
- Castellino S, Groseclose MR, Wagner D. MALDI imaging mass spectrometry: bridging biology and chemistry in drug development. *Bioanalysis.* 2011; 3: 2427-2441. <https://goo.gl/2SWWKW>
- Schone C, Hofler H, Walch A. MALDI imaging mass spectrometry in cancer research: combining proteomic profiling and histological evaluation. *Clin Biochem.* 2013; 46: 539-545. <https://goo.gl/76i6IT>
- Marko Varga G, Fehniger TE, Rezeli M, Dome B, Laurell T, Vegvari A. Drug localization in different lung cancer phenotypes by MALDI mass spectrometry imaging. *J Proteomics.* 2011; 74: 982-992. <https://goo.gl/eA1xXb>
- Hardesty WM, Kelley MC, Mi D, Low RL, Caprioli RM. Protein signatures for survival and recurrence in metastatic melanoma. *J Proteomics.* 2011; 74: 1002-1014. <https://goo.gl/yxEMMz>
- Rauser S, Marquardt C, Balluff B, Albers C, Belau E, Hartmer R, et al. Classification of HER2 Receptor Status in Breast Cancer Tissues by MALDI Imaging Mass Spectrometry research articles. *J Proteome Res.* 2010; 9: 1854-1863. <https://goo.gl/GMjmfq>
- Casadonte R, Kriegsmann M, Zweynert F, Friedrich K, Baretton G, Otto M, et al. Imaging mass spectrometry to discriminate breast from pancreatic cancer metastasis in formalin-fixed paraffin-embedded tissues. *Proteomics.* 2014; 14: 956-964. <https://goo.gl/Ajusd5>



8. Djidja M, Claude E, Snel MF, Francese S, Scriven P, Carolan V, et al. Novel molecular tumour classification using MALDI - mass spectrometry imaging of tissue micro-array. *Anal Bioanal Chem.* 2010; 397: 587-601. <https://goo.gl/jbMXmU>
9. Lossos IS, Morgensztern D. Prognostic biomarkers in diffuse large B-cell lymphoma. *J Clin Oncol.* 2006; 24: 995-1007. <https://goo.gl/eWtMvn>
10. Tilly H, Dreyling M. Diffuse large B-cell non-Hodgkin's lymphoma: ESMO clinical recommendations for diagnosis, treatment and follow-up. *Ann Oncol.* 2009; 20. <https://goo.gl/Ur7X3b>
11. Klapper W, Kreuz M, Kohler CW, Burkhardt B, Szczepanowski M, Salaverria I, et al. Patient age at diagnosis is associated with the molecular characteristics of diffuse large B-cell lymphoma. *Blood.* 2012; 119: 1882-1887. <https://goo.gl/vmUHLy>
12. Alizadeh AA, Eisen MB, Davis RE, Ma C, Lossos IS, Rosenwald A, et al. Distinct types of diffuse large B-cell lymphoma identified by gene expression profiling. *Nature.* 2000; 403: 503-511. <https://goo.gl/amDp3M>
13. Choi WWL, Weisenburger DD, Greiner TC, Piris MA, Banham AH, Delabie J, et al. A New Immunostain Algorithm Classifies Diffuse Large B-Cell Lymphoma into Molecular Subtypes with High. *Clin Cancer Res.* 2009; 15: 5494-5503. <https://goo.gl/2JannG>
14. Meyer PN, Fu K, Greiner TC, Smith LM, Delabie J, Gascoyne RD, et al. Immunohistochemical Methods for Predicting Cell of Origin and Survival in Patients With Diffuse Large B-Cell Lymphoma Treated With Rituximab. *J Clin Oncol.* 2011; 29: 200-207. <https://goo.gl/K1s6Nj>
15. Hans CP, Weisenburger DD, Greiner TC, Gascoyne RD, Delabie J, Ott G, et al. Confirmation of the molecular classification of diffuse large B-cell lymphoma by immunohistochemistry using a tissue microarray. *Blood.* 2004; 103: 275-282. <https://goo.gl/trvVAz>
16. Gustafsson JOR, Eddes JS, Meding S, Koudelka T, Oehler MK, Mccoll SR, et al. Internal calibrants allow high accuracy peptide matching between MALDI imaging MS and LC-MS / MS. *J Proteomics.* 2012; 75: 5093-5105. <https://goo.gl/oBcssx>
17. Barbini L, Rodri J, Dominguez F, Vega F. Glyceraldehyde-3-phosphate dehydrogenase exerts different biologic activities in apoptotic and proliferating hepatocytes according to its subcellular localization. *Mol Cell Biochem.* 2007; 300: 19-28. <https://goo.gl/9a2uJt>
18. Davis RE, Brown KD, Siebenlist U, Staudt LM. Constitutive Nuclear Factor KB Activity Is Required for Survival of Activated B Cell - like Diffuse Large B Cell Lymphoma Cells. *J Exp Med.* 2001; 194: 1861-1874. <https://goo.gl/3tGX44>
19. Compagno M, Lim WK, Grunn A, Nandula S V., Brahmachary M, Shen Q, et al. Mutations of multiple genes cause deregulation of NF- κ B in diffuse large B-cell lymphoma. *Nature.* 2009; 459: 717-721. <https://goo.gl/nzU1pJ>
20. Pancholi V. Multifunctional alpha-enolase: its role in diseases. *Cell Mol Life Sci.* 2001; 58: 902-920. <https://goo.gl/oiNhAP>
21. Diaz Ramos A, Roig-borrellas A, Garc A, Roser L. α -Enolase, a Multifunctional Protein : Its Role on Pathophysiological Situations. *J Biomed Biotechnol.* 2012; 2012.
22. Kumari S, Malla R. New Insight on the Role of Plasminogen Receptor in Cancer Progression. *Cancer Growth Metastasis.* 2015; 8: 35-42. <https://goo.gl/c9XxKc>
23. Capello M, Ferri-borgogno S, Cappello P, Novelli F. a -enolase : a promising therapeutic and diagnostic tumor target. *FEBS J.* 2011; 278: 1064-1074.
24. Song Y, Luo Q, Long H, Hu Z, Que T, Zhang X, et al. Alpha-enolase as a potential cancer prognostic marker promotes cell growth, migration, and invasion in glioma. *Mol Cancer.* 2014; 13: 1-12. <https://goo.gl/5a1XwL>
25. Hsiao K, Shih N, Fang H, Huang T, Kuo C, Elisa A. Surface a -Enolase Promotes Extracellular Matrix Degradation and Tumor Metastasis and Represents a New Therapeutic Target. *PLoS One.* 2013; 8: e69354.
26. Schmitt E, Gehrmann M, Brunet M, Multhoff G, Garrido C. Intracellular and extracellular functions of heat shock proteins: repercussions in cancer therapy. *J Leukoc Biol.* 2007; 81: 15-27. <https://goo.gl/GuBy5M>
27. Luk JM, Lam C, Siu AFM, Lam BY, Ng IOL, Hu M, et al. Proteomic profiling of hepatocellular carcinoma in Chinese cohort reveals heat-shock proteins (Hsp27, Hsp70, GRP78) up-regulation and their associated prognostic values. *Proteomics.* 2006; 6: 1049-1057. <https://goo.gl/pt2zZm>
28. Gyrd hansen M, Nylandsted J, Jaattela M. Heat Shock Protein 70 Promotes Cancer Cell Viability by Safeguarding Lysosomal Integrity. *Cell cycle.* 2004; 3: 1484-1485. <https://goo.gl/XL4XeK>
29. Ciocca DR, Calderwood SK. Heat shock proteins in cancer: diagnostic, prognostic, predictive, and treatment implications. *Cell Stress Chaperones Cell Stress Soc Int.* 2005; 10: 86-103. <https://goo.gl/TepbLy>
30. Kreunin P, Yoo C, Urquidi V, Lubman DM. Differential expression of ribosomal. *Cancer genomics proteomics.* 2007; 4: 329-339. <https://goo.gl/h87ATq>
31. Hagner PR1, Mazan-Mamczarz K, Dai B, Balzer EM, Corl S, Martin SS, et al. Ribosomal protein S6 is highly expressed in non-Hodgkin lymphoma and associates with mRNA containing a 5' terminal oligopyrimidine tract. *Oncogene.* 2011; 30: 1531-1541. <https://goo.gl/4WQkjN>
32. Wool IG. Extraribosomal functions of ribosomal proteins. *TIBS.* 1996; 21: 164-165. <https://goo.gl/tFWxfX>
33. Warner JR, Mcintosh KB. How common are Extra-ribosomal Functions of Ribosomal Proteins. *Mol Cell.* 2009; 34: 3-11. <https://goo.gl/gzdgw6>
34. Barnard G, Mori M, Staniunas R, Begum N, Bao S, Puder M, et al. Ubiquitin fusion proteins are overexpressed in colon cancer but not in gastric cancer. *Biochim Biophys Acta.* 1995; 1272: 147-153. <https://goo.gl/BD47fs>
35. Mafune K, Wong JM, Staniunas RJ, Lu ML, Ravikummar TS, Chen LB, et al. Ubiquitin hybrid protein gene expression during human colon cancer progression. *Arch Surg.* 1991; 126: 462-466. <https://goo.gl/JhgSZn>
36. Seeley EH, Caprioli RM. Molecular imaging of proteins in tissues by mass spectrometry. *Proc Natl Acad Sci U S A.* 2008; 105: 18126-18131. <https://goo.gl/hy7j3C>
37. Seeley EH, Caprioli RM. MALDI imaging mass spectrometry of human tissue: method challenges and clinical perspectives. *Trends Biotechnol.* 2011; 29: 136-143. <https://goo.gl/w1FTk2>